Degradation and Mineralization of Metformin by Electro-Oxidation on Ti/DSA (Ta_2O_5-Ir_2O_5) Anode and Combined Electro-Oxidation and Electro-Coagulation on Stainless Steel (SS) Anode

Meena, Vinod Kumar; Ghatak*+, Himadri Roy

Department of Chemical Engineering, Sant Longowal Institute of Engineering and Technology, Longowal, Sangrur, Punjab, INDIA

ABSTRACT: *We conducted electro-oxidation, and combined electro-oxidation and electro-coagulation batch experiments on synthetic wastewater containing an anti-diabetic drug metformin hydrochloride (MET-HCl). Degradation and mineralization were studied on Ti/DSA (Ta_2O_5-Ir_2O_5) and stainless steel (SS) anodes. Electrochemical behavior was observed by cyclic voltammetry techniques. The effect of applied current density was evaluated at 50 ppm concentration of supporting electrolyte sodium sulphate (Na_2SO_4). Electro-oxidation on Ti/DSA anode resulted in maximum degradation of 94.88% at the corresponding specific charge (Q) of 2.1 Ah/L, current density of 0.93 mA/cm^2 and Na_2SO_4 concentration of 100 ppm. Similarly, maximum mineralization obtained was 70.64% at corresponding specific charge (Q) of 2.1 Ah/L, current density of 0.93 mA/cm^2 and Na_2SO_4 concentration of 50 ppm. Energy consumption was 2081.56 kWh/kgTOC. Further, under identical conditions, combined electro-oxidation and electro-coagulation on SS anode resulted in maximum degradation of 99.48% at corresponding specific charge (Q) of 2.1 Ah/L, current density of 0.93 mA/cm^2 and Na_2SO_4 concentration of 100 ppm. Similarly, maximum mineralization obtained was 99.04% at corresponding specific charge (Q) of 2.1 Ah/L, current density of 0.93 mA/cm^2, and Na_2SO_4 concentration 75 ppm. Energy consumption was 870.98 kWh/kgTOC.*

KEYWORDS: *Metformin hydrochloride; Electro-oxidation; Electro-coagulation; Degradation; Mineralization; Energy consumption; Mineralization current efficiency.*

INTRODUCTION

Metformin (MET) is used as the first-line drug for treating type 2 diabetes worldwide [1] and it is termed a biguanide antihyperglycaemic agent in terms of pharmacology. Polycystic ovarian syndrome (PCOS) can also be treated by MET [2]. MET is reported as one of the most used medical prescription drugs worldwide [4]. MET as the first line of the hypoglycaemic is considered to diminish plasma glucose levels via enhancing insulin sensitivity and decreasing hepatic glucose release. Currently, MET, is the only biguanide available in the

* *To whom correspondence should be addressed.*
+E-mail address: h_r_ghatak@yahoo.com
1021-9986/2022/12/3972-3987 16/$/6.06

United States which does not cause weight gain and hypoglycaemia, unlike the insulin secretagogues. In recent years the presence of MET has been detected in natural waterbodies with maximum concentrations of 1.58, 2.64, and 222.10 μg/L, respectively, in groundwater, surface water, and wastewater [4-6]. MET has been detected in sludge in a recent study with a maximum concentration of 2960 ng/g [7-8]. MET concentration in a range of 0.06–3.1 g/L in surface water and 1.2–118 g/L in Water and WasteWater Treatment Plants (WWTPs) was reported by other researchers [6, 9-11]. MET is reportedly introduced into the environment in both metabolized (guanyl urea) and non-metabolized forms through domestic, hospital, and pharmaceutical industry wastewater [12]. MET and GUA have been considered emerging micropollutants due to their high consumption and reported eco-toxicity.

Pharmaceuticals generally dissolve easily in aqueous media and they do not usually evaporate at normal temperatures or pressure. Due to this fact, they make their way into the aquatic environment and soil via treated sewage sludge (biosolids), sewage, and also by irrigation with reclaimed waters [13, 14]. It is demonstrated by current research findings that pharmaceuticals and/or their metabolites and their degradation by-products are not sufficiently removed from wastewater and therefore they reach the surface, ground, marine, and drinking waters [15-17]. Although MET's potential degradation to dead-end metabolite, GUA in activated sludge was reported, it is still detected at high concentrations in surface water and effluent due to its high influent load [9]. Recent studies have shown that MET can be taken up by vegetables and crops and also accumulate in leaves) [18, 19]. Reported effects from long-term exposure to different Pharmaceutically Active Compounds (PhACs) include endocrine disruption, gene toxicity, carcinogenicity, antibiotic resistance initiation in human pathogens, allergic reactions, and reproductive effects [20-22]. MET has been identified as an endocrine disruptor to fish and is of immediate concern [23] at environmentally relevant concentrations (40 μg/L). The effect on microbial communities of long-term exposure to MET and their ability to degrade metformin or its transformation product GUA is known very little [24].

In the closed bottle test (OECD301D) MET is classified as not readily biodegradable despite its reported biodegradation in WWTPs. In the Manometric Respiratory test (OECD 301F), MET also showed signs of elimination in one of three bottles with degradation up to 48.7%. MET's partial degradation in the Zahn-Wellens test (OECD 302B) was also reported in both replicates with the elimination of 51.3 and 49.9% [25]. Due to MET and its metabolite GUA's physical-chemical properties, obstruction is reported in the trace-analysis by conventional treatment methods which resulted in poor recoveries during the solid-phase extraction process and also resulted in no retention during chromatographic separation [15, 26, 27]. Recalcitrant PhACs which may include reactants, Active Pharmaceutical Ingredients (APIs), organic solvents, and reactants, and raw materials are unable to completely degraded by biological treatments [28-30]. Advanced oxidation like ozonation has the drawback of high cost and the need of adding hazardous oxidant from outside [31]. Photo catalytic degradation processes are plagued by low quantum efficiencies and resultant high energy consumption [32]. Recently, Graphene oxide was also used for the efficient removal of MET from water [2]. Nevertheless, the MET showed high bio-persistence and also having the potential to cause gene damage, lung cancer and induced sustained inflammation [2, 33]. Therefore, for the removal of MET from wastewater, an efficient and environmentally friendly method is to be implemented. MET degradation in aqueous solutions by electro-activation of persulfate and hydrogen peroxide using natural and synthetic ferrous ion sources, was reported in literature [12]. Nickel oxide nanotubes carbon micro-particles/Nafion nanocomposites for the electro-oxidation of MET were also reported in the literature [34].

To the best of our knowledge and based on the literature, there is no previous report on the degradation and mineralization of MET by electro-oxidation on Ti/DSA (Ta_2O_5-Ir_2O_5) anode and combined electro-oxidation and electro-coagulation on SS anode. Electrochemical processes are found effective and also known as green technology for the decomposition of organic pollutants on some dimensionally stable anodes as well [44]. Electrochemical advanced oxidation processes are having advantages over other advanced oxidation processes, such as the recoverability of electrochemical sludge, low operational costs with significant mineralization of organic pollutants [12]. Ti/DSA electrodes were reported in electrochemical oxidation and they had high efficiency and stability in wastewater treatment of refractory molecules [35]. Moreover, titanium plates were also reported as more suitable

because of their inexpensiveness and non-toxicity [36]. Titanium dioxide modified with metal oxide has been used in the degradation of formic acid wherein it showed a synergetic effect on catalyst activity [37-38]. Stainless steel is chosen as the electrode material for the combined process. Previous studies suggest its effectiveness in the mineralization of diclofenac sodium through the combined process of electro-oxidation and electro-coagulation [39]. Electrooxidation, though demanding in terms of electrical energy, is an attractive treatment method as no oxidant is to be added from outside. Further, the utilization of cathodic hydrogen through process integration can reduce overall energy consumption [40].

This study reports the degradation and mineralization of MET-HCl using the process of electro-oxidation on Ti/ DSA (Ta_2O_5-Ir_2O_5) and combined electro-oxidation and electro-coagulation on SS anode. The effect of different process parameters is studied. The two processes are compared for their effectiveness in degrading and mineralizing MET-HCl as well as the energy dynamics.

EXPERIMANTAL SECTION

Chemicals and reagents

MET-HCl ($C_4H_{11}N_5$.HCl) of pharmaceutical standard, used in the study, was kindly donated by M/s IOLCP, Barnala, India. It was used as the target organic pollutant. Ti/DSA (Ta_2O_5-Ir_2O_5) plates (50mm×45mm×1mm thick with Hook 60mm×8mm×1mm thick) were procured from Ti Anode Fabricator Pvt. Ltd., Chennai, India. SS 304 (50mm×45mm×1mm thick with Hook 60mm×8mm×1mm thick) was procured from a local metal shop in Sangrur, India. Sodium carbonate anhydrous (Na_2CO_3) and sodium hydrogen carbonate ($NaHCO_3$) of AR grades were purchased from CDH, Mumbai, India. Orthophosphoric acid (H_3PO_4) and potassium hydrogen phthalate ($C_8H_5KO_4$) of HPLC grade were purchased from Loba Chemie Pvt. Ltd., Mumbai, India. Sodium Lauryl sulfate ($NaC_{12}H_{25}SO_4$) SQ grade was purchased from Qualigens Fine Chemicals, Mumbai, India. Potassium dihydrogen orthophosphate (KH_2PO_4) purified purchased from SD Fine Chem Limited, Mumbai, India. Sodium sulfate (anhydrous) of SQ grade was purchased from Thermo Fisher Scientific India Pvt. Ltd, Mumbai, India. All the solutions were prepared with ultrapure deionized water obtained with a Millipore water purification system (Merck progard® TS2).

Voltammetry experiments

Electrochemical measurements were carried out using a conventional three-electrode cell with a capacity of 80mL in conjunction with a computer-controlled potentiostat/galvanostat model SP-150 with EC Lab V10.33 software. Ti/DSA and SS-304 electrodes having an effective surface area 2 cm^2 were used as the working electrode, Mercury/Mercurous Sulfate (MMS) as a reference electrode, and platinum wire coil as the counter electrode. Voltammetry experiments were performed in unstirred solutions at scan rates of 10, 50, 100, and 200 mv/s. Voltammograms were recorded after 10 cycles.

Electro-oxidation and combined electro-oxidation and electro-coagulation

The degradation and mineralization of the MET-HCl was carried out in a glass reactor of 250 mL . Ti/DSA was used as the anode and SS-304 was used as cathode for the electro-oxidation experiments, whereas SS-304 electrode was used as anode as well as cathode for the combined electro-oxidation and electro-coagulation experiments. Both electrodes were rectangle shaped with each having working area of 90 cm^2 and a 5 mm inter-electrode gap was used.

All experiments were performed using 200 mL synthetic wastewater containing 50 ppm of MET-HCl at 3 different supporting electrolyte concentrations of 50, 75 and 100 ppm of Na_2SO_4 at three current densities of 0.67, 0.93 and 1.16 mA/cm^2. 2mL samples were withdrawn through a syringe filter at different intervals and used for analytical purposes. All experiments were performed in duplicate and the average results were reported.

Analytical methods

Total Organic Carbon (TOC) was determined using a TOC-L Shimadzu, TOC analyzer, based on combustion catalytic oxidation. The concentration of MET-HCl after the treatment was measured by HPLC system consisting of a pump (Waters 1515 isocratic pump). The detector used was Waters 2487 (dual λ detector). The wavelength was set at 233 nm. The software used was Breeze. The column used was Atlantis HILIC (Silica 5µm 4.6×250 mm) working on the opposite principle of Reverse phase chromatography. The mobile phase contained acetonitrile (34%) and an aqueous phase (66%).

The aqueous phase contained 10 mM Potassium dihydrogen orthophosphate KH_2PO_4 and 10mM sodium

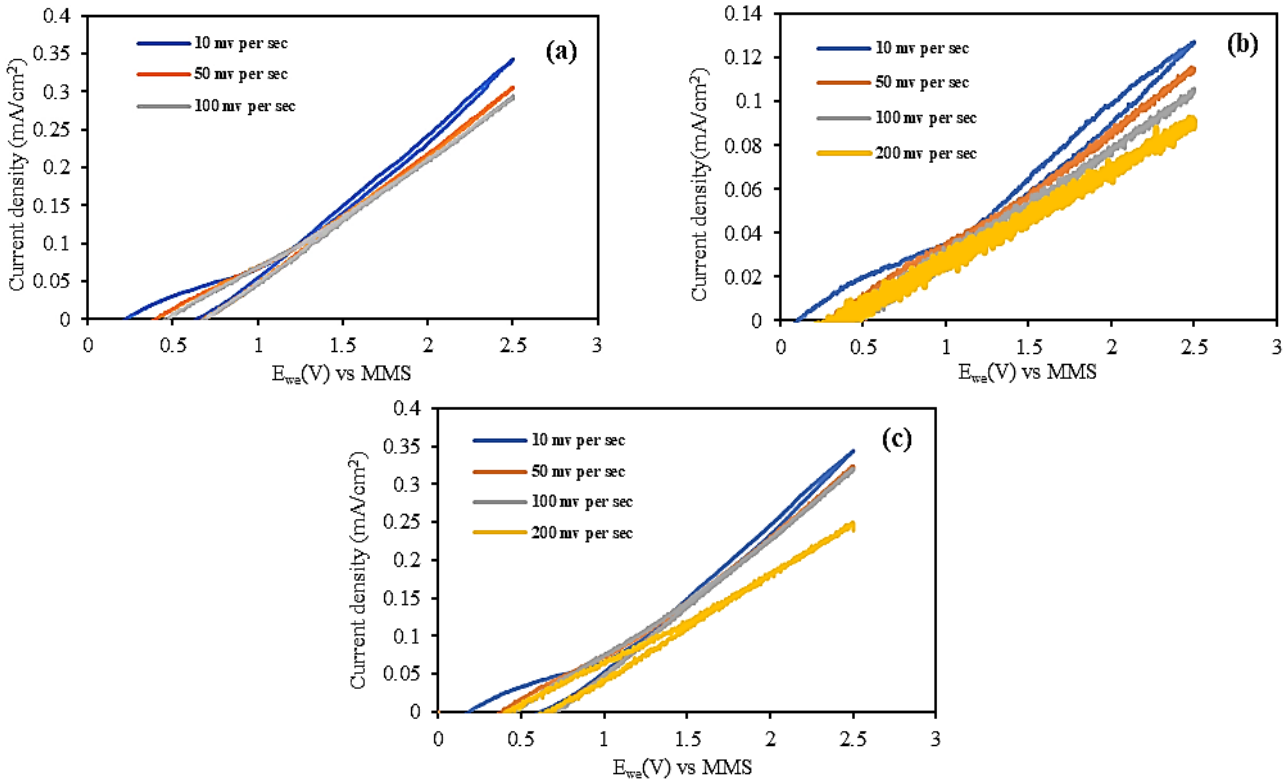

Fig. 1: Cyclic voltammograms of Ti/DSA anode of (a) 50 ppm Na_2SO_4 (b) 50 ppm MET-HCl (c) solution of 50 ppm MET-HCl and 50 ppm Na_2SO_4 at 10, 50, 100 and 200 mV/s scan rates; 0→2.5 V vs. MMS.

lauryl sulfate. Dilute orthophosphoric acid was used to adjust the pH of the aqueous phase to 5.2. The mobile phase was run isocratically and the flow rate was maintained at 1.3 mL /min. Injection volumes were 20µL.

RESULTS AND DISCUSSION

Electro-oxidation of MET-HCl

Electrochemical measurements

To characterize the electrode, it is important to determine the potential window and the oxygen evolution reaction by electrochemical measurements at the Ti/DSA electrode**.** Before starting the MET-HCl degradation, cyclic voltammetry experiments were performed in the potential region of 0 to 2.5 V vs Hg/Hg_2SO_4 (MMS) reference electrode to achieve information regarding the MET-HCl electro-oxidation mechanism (direct or indirect). The potential range was chosen based on reported studies on electro-oxidation systems that used Na_2SO_4 as a supporting electrolyte [41]. The cyclic voltammograms shown in Fig. 1 were obtained in aqueous solutions of (i) 50 ppm MET-HCl and 50 ppm Na_2SO_4, (ii) 50 ppm Na_2SO_4, and (iii) 50 ppm MET-HCl, at different scan rates of 10, 50, 100 and 200 mv/sec.

No electro-oxidation peaks were observed in any voltammogram. In Fig.1 (a) and (b), an anodic shoulder could be observed near 1.2 V vs Hg/Hg_2SO_4 arising from the oxidation of the supporting electrolyte to persulfate ions sulfate radicals ($SO_4^{\bullet-}$). At higher potentials, oxygen evolution set in, and current density increased sharply. Similar behavior is reported by other researchers on aqueous systems containing Na_2SO_4 on different anodes [40]. It is evident that Met-HCl does not undergo direct anodic electro-oxidation in this potential window. It is further revealed in Fig. 1 (a) and (b) that the current density approaches up to 0.35 mA/cm^2 when Na_2SO_4 is present in the system. In comparison, the maximum current density was only about 0.12 mA/cm^2 when Na_2SO_4 was absent. This brings forth the role of supporting electrolytes in boosting the conductivity of the solution.

Cyclic voltammograms of MET-HCl and Na_2SO_4 on Ti/DSA anode are lacking in the literature. The result has shown the probable formation of sulfate radicals ($SO_4^{-}\cdot$) which could transform tinto persulfate ions ($S_2O_8^{2-}$) in the presence of hydroxyl radicals ($HO\cdot$) as represented in reactions (1) through (3) [40-42].

Table 1: First order rate kinetics of electro-oxidation of MET-HCl at Ti/DSA anode.

Current density (mA/cm^2)	Na_2SO_4 concentration (ppm)	value of rate constant k (L/Ah)
Mineralization		
0.67	50	0.5795
0.93	50	0.6099
1.16	50	0.4680
0.93	75	0.3981
0.93	100	0.3879
Degradation		
0.67	50	1.3458
0.93	50	1.1208
1.16	50	0.9244
0.93	75	1.3936
0.93	100	1.4243

$$H_2O \rightarrow HO\cdot + H^+ + e^- \quad (1.76\text{-}2.26V \text{ vs MMS}) \quad (1)$$

$$HSO_4^- + HO\cdot \rightarrow SO_4^{-}\cdot + H_2O \quad (2)$$

$$2\ SO_4^{-}\cdot \rightarrow S_2O_8^{2-} + 2e^- \quad (1.46V \text{ vs MMS}) \quad (3)$$

Therefore, it is necessary to consider that the oxidation of MET-HCl on Ti/DSA results from indirect oxidation involving persulfate ions and sulphate radicals along with hydroxyl radicals.

Effect of applied current density

We evaluated the effect of current density by performing electro-oxidation experiments on 50 ppm MET-HCl solution supported with 50 ppm Na_2SO_4 as an electrolyte at current densities of j_{app} 0.67, 0.93 and 1.16 mA/cm^2.

For the Ti/DSA anode, Fig. 2a shows the effect of current density on the progressive degradation of MET-HCl as relative concentration plotted as a function of Specific charge. An excellent linear fit between the natural logarithm of C_t/C_o against Specific charge, shown in Fig. 2b, confirms that degradation follows pseudo-first-order kinetics. At the beginning of electro-oxidation (moderate values of specific charge), we observed high rates of degradation at each current density indicating efficient utilization of the oxidant radicals. The degradation rate decreased with a specific charge, primarily due to the ever-decreasing residual concentration of MET-HCl. At each current density, degradation of MET-HCl increased continuously with respect to specific charges for the entire duration of electrolysis treatment. The decay of MET-HCl depended on the current density, and it increased from 85.56 to 89.62% as current density increased from 0.67 to 0.93 mA/cm^2; corresponding specific charge values were 1.5 and 2.1 Ah/L, respectively. It further increased from 89.62 to 90.40% as current density increased from 0.93 to 1.16 mA/cm^2 with the corresponding specific charge increasing to 2.6 Ah/L. For kinetics analysis, the MET-HCl removal rate was calculated by a pseudo-first-order equation as follows [12]:

$$\text{Ln}\ (C_t/C_o) = -kQ \quad (4)$$

Here, C_t = residual MET-HCl concentration, C_0 = initial MET-HCl concentration, k= pseudo first order rate constant (L/Ah), Q = specific charge (Ah/L).

We observed a decrease in the pseudo first order rate constant when current density first increased from 0.67 to 0.93 mA/cm^2 but thereafter the rate constant decreased as the current density was further increased to 1.16 mA/cm^2. These are shown in Table 1. Here, there is an apparent paradox. With increasing current density, oxidant radicals will form rapidly. At the same time, the electro-oxidation will be carried out at increased potentials as depicted in Fig. 1. This would promote oxygen evolution as a side reaction. This flattens the net rate of production of oxidant radicals causing a drop in rate constant.

Fig. 2c shows the effect of the current density on the decay of the relative TOC concentration as a function of Specific charge (Ah/L) for the Ti/DSA Anode. Fig. 2d shows the effect of the current density on the linear variation of the natural logarithm of TOC_t/TOC_0 as a function of Specific charge (Ah/L) for the Ti/DSA Anode. This confirmed adherence to pseudo-first-order kinetics for mineralization as well. The decay of relative Mineralization, as measured by TOC concentration of MET-HCl, depended on the current density. It increased from 55.27 to70.64% when the current density increased from 0.67 to 0.93 mA/cm^2 but reduced thereafter to 68.16% when the current density increased to 1.16 mA/cm^2. The corresponding specific charge values were 1.5, 2.1, and 2.6 Ah/L, respectively. There was a very marginal (about 5%) increase in pseudo-first-order rate constant with current density increasing from 0.67 to 0.93 mA/cm^2. However the rate constant significantly dropped (23%) when the current density increased further to 1.16 mA/cm^2. These are shown in Table 1. Hence, it is important to note that when the current density exceeds a certain value – in this case from 0.93 to 1.16 mA/cm^2 – the mineralization efficiency (TOC removal) and the pseudo-first-order rate

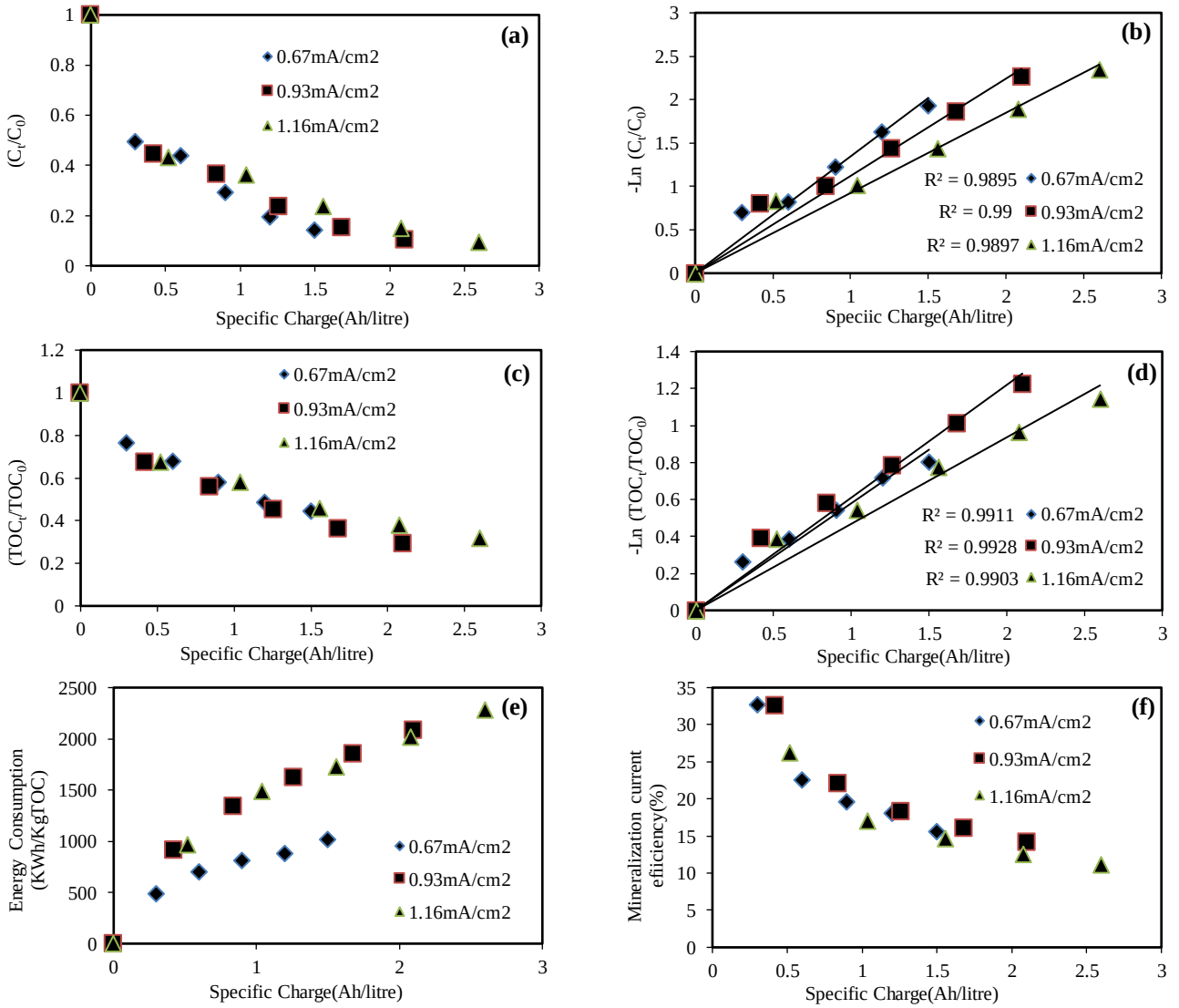

Fig. 2: Effect of the current density and specific charge (Ah/L) for the electro-oxidation of MET-HCl on Ti/DSA anode (a) relative MET-HCl concentration (b) ln(Ct/C0) (c) relative TOC (d) ln(TOCt/TOC0) (e) EC (f) MCE. Conditions: 50 ppm MET-HCl, 50 ppm Na_2SO_4

constant decreases. This could be attributed to oxygen evolution side reaction at higher current densities.

$$2H_2O \rightarrow O_2 + 4H^+ + 4e^- \quad (5)$$

Production of a greater amount of gas at the surface of the electrode also masks the anode's active sites [43], further suppressing the generation of hydroxyl radicals. As explained, oxidant species such as $S_2O_8^{2-}$ and $SO_4^{\cdot-}$ are also formed according to reactions (2) and (3). All this has the effect of reducing the HO• concentration, the strongest oxidant species, replacing it with relatively weaker oxidants like $S_2O_8^{2-}$ and $SO_4^{\bullet-}$. Fig. 2e shows the effect of the current density on the energy consumption (EC) as a function of the specific charge (Ah/L) for the Ti/DSA anode. EC (kWh/kgTOC) was calculated with eq^n (6) [44].

$$EC = \frac{1000\ UIt}{(TOC0-TOCt)V} \quad (6)$$

Here, U = voltage of the cell in volts (V), t = reaction time in hour (h), I = applied current in amperes (A), V = cell volume (L), TOC_0 and TOC_t are the initial concentration of TOC (mg /L) and concentration at time t.

At each current density, EC increased continuously with respect to specific charge for the entire duration of electro-oxidation. EC increased from 1017.46 to 2081.56 and then to 2281.90 kWh/kgTOC as current density increased from 0.67 to 0.93 and then to 1.16 mA/cm^2. Corresponding specific

charge values were 1.5, 2.1, and 2.6 Ah/L, respectively. Higher current density accelerated the side reactions such as the formation of O_2 by eq^n (5), leading to a larger proportion of specific charge being consumed in these side reactions. This is reflected in the form of higher Ec [45-46].

Fig. 2f shows the effect of the current density on the mineralization current efficiency (MCE) as a function of Specific charge (Ah/L) for the Ti/DSA anode. The MCE as a percentage was calculated from eq^n (7) [44]

$$MCE = \frac{nFV\Delta\, TOC}{4.32\times107\ mIt}\times100\% \quad (7)$$

Here, F = Faraday constant (96487 C/mol), V = volume of solution (L), Δ TOC= ΔTOC is the measured TOC removal (mg/L) after a certain time t (h), 4.32×10^7 = conversion factor [3600 (s/h) × 12000 mg of (C/mol)], m = number of carbon atom of MET-HCl (4C atoms), n = number of electrons consumed per molecule of MET-HCl into CO_2 and NO_3^- in eq^n (8) is 52.

$$C_4H_{11}N_5.HCl + 23\ H_2O \rightarrow 4CO_2 + 5NO_3^- + 52e^- + 58\ H^+ + Cl^- \quad (8)$$

At each current density, MCE decreased with a progressive increase in electro-oxidation-specific charge. This is due to the declining concentration of MET-HCl and the increasing recalcitrance of intermediates. MCE decreases with the specific charge at each current density. As current density increased from 0.67 to 0.93, and then to 1.16 mA/cm^2 the final MCE first decreased from 15.52 to 14.17% and then further dropped to 11.04%. It is because the hydroxyl radicals formed are rapidly destroyed by side reactions resulting in its lesser availability for the reaction with organics and consequently MCE is also decreased. These reactions could be expressed as [47]

$$\text{MET-HCl}(\cdot OH) \rightarrow \text{MET-HCl} + \frac{1}{2}O_2 + H^+ + e^- \quad (9)$$

$$2\ \text{MET-HCl}(\cdot OH) \rightarrow 2\text{MET-HCl} + H_2O_2 \quad (10)$$

$$H_2O_2 + \text{MET-HCl}(\cdot OH) \rightarrow \text{MET-HCl}(HO_2\cdot) + H_2O \quad (11)$$

Influence of supporting electrolyte concentration

Fig. 3a shows the effect of the Na_2SO_4 concentration on MET-HCl degradation. To elucidate the kinetics, integral method of analysis was applied and presented in Fig. 3b. Natural logarithm of C_t/C_o when plotted against Specific charge, provided a straight line functionality with high correlation coefficients for the Ti/DSA anode. This confirms pseudo first order kinetics for all supporting electrolyte concentrations. Degradation rate steadily decreased with a specific charge for all supporting electrolyte concentrations. The decay of the MET-HCl depended on the supporting electrolyte concentration. It increased from 89.62 to 94.50% as Na_2SO_4 concentration increased from 50 to 75 ppm. But the further increase in Na_2SO_4 concentration from 75 to 100 ppm resulted in only a marginal increase in degradation of 94.50 to 94.88% which is rather insignificant. With more Na_2SO_4, solution conductivity increases favoring the movement of ions. The pseudo-first-order rate constant was found to increase with Na_2SO_4 concentration increasing from 50 to 100 ppm. These rate constants are shown in Table 1.

The effect of Na_2SO_4 concentration on mineralization kinetics was analyzed by integral method. Fig. 3c is a plot of the relative TOC concentration as a function of Specific charge (Ah/L) for the Ti/DSA Anode. Fig. 3d shows the integral form of the pseudo first-order rate equation with respect to specific charges. High correlation confirms pseudo-first-order kinetics on Ti/DSA anode. Mineralization, as measured by the decrease in relative TOC concentration, was found to decrease from 70.64 to 53.62% as Na_2SO_4 concentration was increased from 50 to 75 ppm. Mineralization further decreased from 53.62 to 52.93% as Na_2SO_4 concentration increased from 75 to 100 ppm. The corresponding specific charge was 2.1 Ah/L. The pseudo-first-order mineralization rate constant decreased when Na_2SO_4 concentration was increased from 50 to 100 ppm, as shown in Table 1. With the increase in the Na_2SO_4 concentration, TOC abatement of MET-HCl was decreased as more SO_4^{2-} would move to the anode under the influence of the electric field and compete for the transferred charge with the water-splitting reaction. This will more than offset the effect of increased solution conductivity causing a decrease in mineralization.

Fig. 3e shows the effect of the Na_2SO_4 concentration on the EC as a function of Specific charge (Ah/L) for the Ti/DSA anode. At each Na_2SO_4 concentration, EC increased continuously with respect to specific charges. As Na_2SO_4 concentration increased from 50 to 75 ppm, the EC decreased from 2081.56 to 1684.32 kWh/kg TOC. Similarly, when Na_2SO_4 concentration was increased from 75 ppm to 100 ppm, the EC further decreased from 1684.32 to 1646.09 kWh/kg TOC. Higher the Na_2SO_4 concentration, lower the cell voltage required to maintain a given current density. This translates into reduced EC.

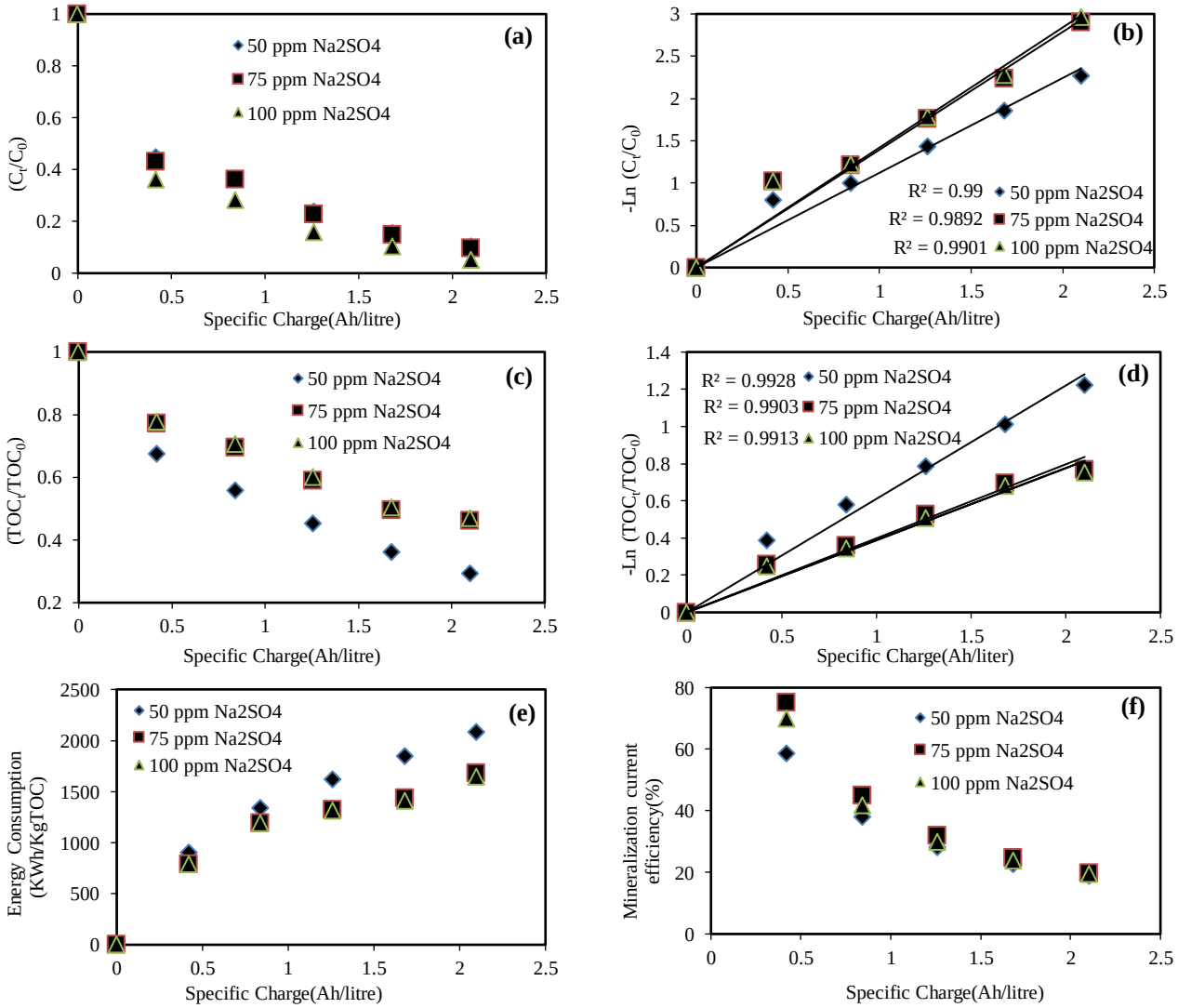

Fig. 3: Effect of Na_2SO_4 concentration and specific charge (Ah/L) on the electro-oxidation of MET-HCl on Ti/DSA anode (a) relative MET-HCl concentration (b) ln(C_t/C_0) (c) relative TOC concentration (d) ln(TOC_t/TOC_0) (e) EC (f) MCE. Conditions: 50 ppm MET-HCl, Current density 0.93 mA/cm^2

Fig. 3f shows the variation of MCE with Specific charge (Ah/L) at different Na_2SO_4 concentrations for the Ti/DSA anode. The reduction of MCE with a specific charge could be related to the formation of the intermediate product that was oxidized with more difficulty by the oxidants, As Na_2SO_4 concentration was increased from 50 to 75 ppm the MCE decreased from 14.17 to 10.76%. Similarly, when Na_2SO_4 concentration was further increased from 75 to 100 ppm, MCE marginally decreased from 10.76 to 10.62%. On one hand, higher Na_2SO_4 concentration suppressed the generation of hydroxyl radicals as SO_4^{2-} would compete for the transferred charge with the water-splitting reaction. On the other hand, more and more hydroxyl radicals formed were destroyed through eq^n (9), (10), and (11) when the Na_2SO_4 concentration increased. That is why this radical's lesser proportion was available for the reaction with organics [47] and consequently, MCE was also decreased. To sum up, it is worthwhile to note that increasing Na_2SO_4 concentration, while suppressing the rate of mineralization and MCE, reduced the EC. This can be important for plant economics.

Combined Electro-oxidation and electro-coagulation of MET-HCl

Electrochemical measurements

Cyclic voltammetry was performed to ascertain the MET-HCl combined electro-oxidation and electro-coagulation mechanism (direct or indirect) on SS anode.

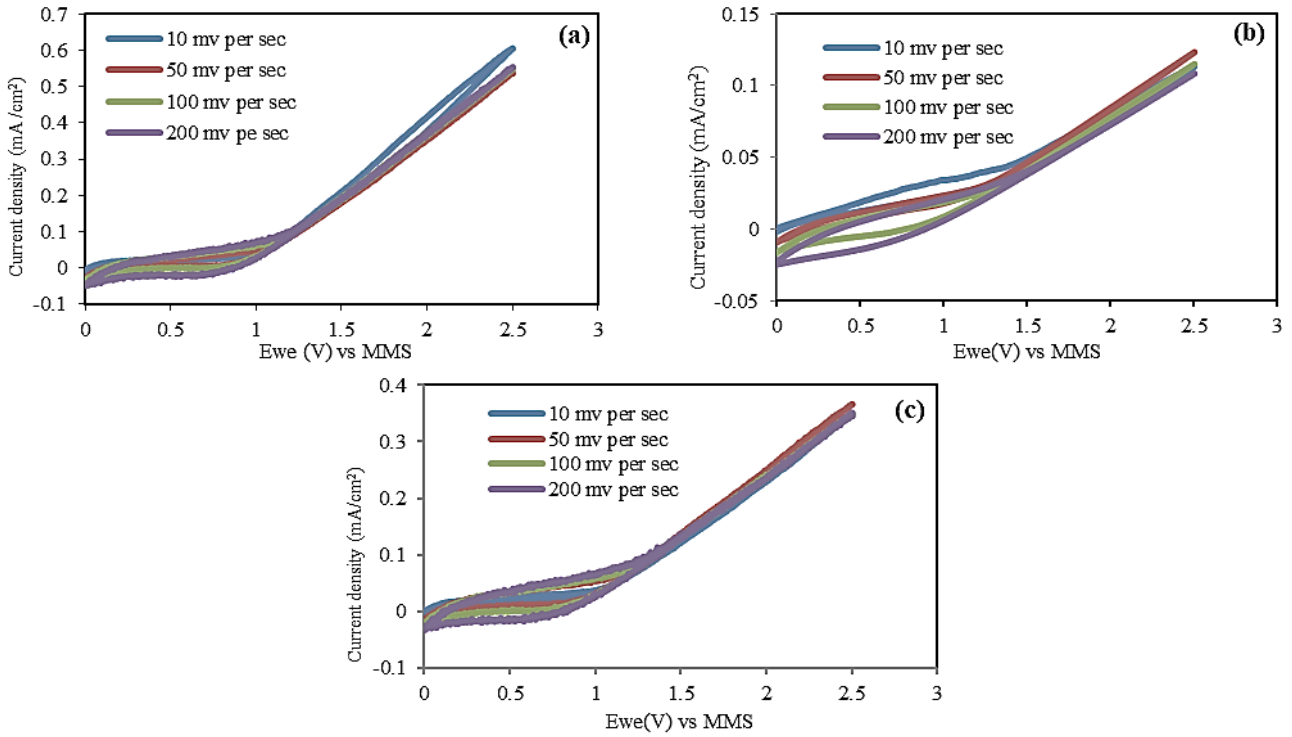

Fig. 4: Cyclic voltammograms of SS anode of (a) 50 ppm Na_2SO_4 (b) 50 ppm MET-HCl (c) solution of 50 ppm MET-HCl and 50 ppm Na_2SO_4 at 10,50,100&200 mV/s scan rates; 0→2.5 V vs. MMS.

The 0 to 2.5 V potential range vs MMS reference electrode was chosen based on earlier work on electrochemical transformation of Na_2SO_4 [41]. Three sets of cyclic voltammetric curves are shown in Fig. 4 each for aqueous solutions of (i) 50 ppm MET-HCl and 50 ppm Na_2SO_4, (ii) 50 ppm Na_2SO_4, and (iii) 50 ppm MET-HCl, at different scan rates of 10, 50, 100 and 200 mv/sec. While no anodic peaks were observed, an anodic shoulder did appear in all voltammograms at close to 1.2 V vs MMS. This behavior is similar to that shown by Ti/DSA. Accordingly, oxidation of the sulphate ions (SO_4^{2-}) to sulphate radicals ($SO_4^{\bullet-}$) and their subsequent oxidation to persulfate ions ($S_2O_8^{2-}$) remains the main charge transfer reaction at lower potential [41]. Finally, oxygen evolution set in and current density increased sharply with increasing potential. As Na_2SO_4 increases the conductivity of the solution we observe higher current density in voltammograms of Fig. 4 for solutions containing Na_2SO_4.

In addition, iron oxidation occurs at the anode at a much lower potential according to the well-known reaction [39]

$$Fe(s) \rightarrow Fe^{2+} + 2e^- \qquad (-1.08V \text{ vs MMS}) \qquad (12)$$

electro-generating ferrous ion Fe^{2+}. These can further oxidize to ferric ions Fe^{3+} according to eq^n (13).

$$Fe^{2+} \rightarrow Fe^{3+} + e^- \qquad (0.13V \text{ vs MMS}) \qquad (13)$$

Coagulants Fe^{2+}, and Fe^{3+} are, therefore, generated in situ which contribute to organics removal. Ferrous ions can react with persulfate ions through the following reaction [12].

$$2Fe^{2+} + S_2O_8^{2-} \rightarrow 2Fe^{3+} + SO_4^{\cdot-} + SO_4^{2-} \qquad (14)$$

Therefore, it is necessary to consider that the electrochemical remediation of MET-HCl on SS anode is not by electro-oxidation alone. Oxidant species including hydroxyl radicals would degrade and ultimately mineralize MET-HCl. In combination, electro-coagulation would also assist its removal by the in situ-generated ferrous and ferric ions.

Effect of applied current density

Progressive degradation of MET-HCl on SS anode is presented in Fig. 5a – a plot between relative MET-HCl concentration and Specific charge (Ah/L) – at different current densities. Integrated pseudo-first-order rate equation – linear plots between the natural logarithm of C_t/C_o and Specific charge – are shown in Fig. 5b. Experimental values correlate well with the regressed straight lines. This confirms that degradation follows pseudo-first-order kinetics even in the combined process of electro-oxidation and electro-coagulation. At each current density degradation of

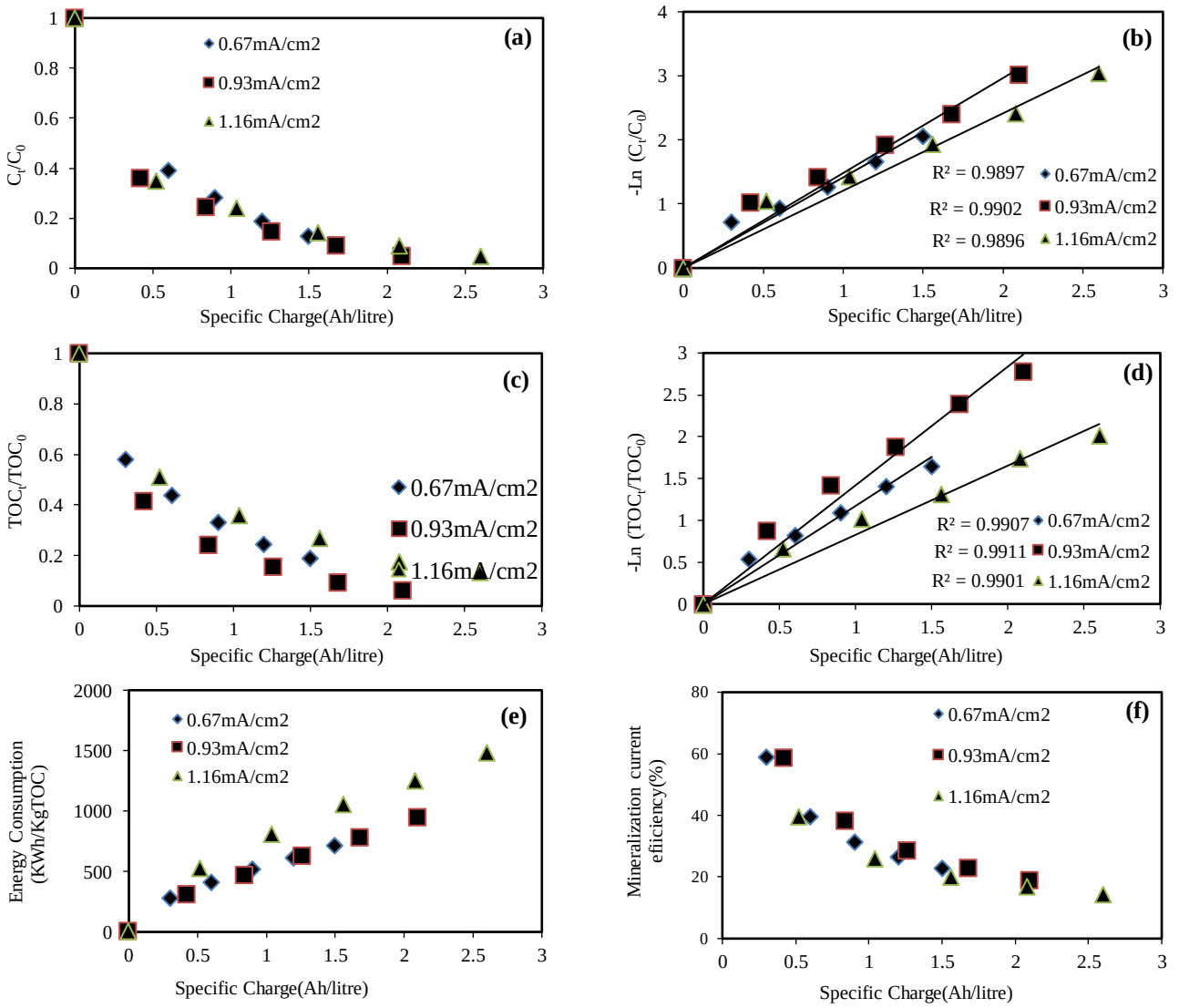

Fig. 5: Effect of the current density and specific charge (Ah/L) for the combined electro-oxidation and electro-coagulation of MET-HCl on SS anode (a) relative MET-HCl concentration (b) ln(C_t/C_0) (c) relative TOC (d) ln (TOC_t/TOC_0) (e) EC (f) MCE. Conditions: 50 ppm MET-HCl, 50 ppm Na_2SO_4

MET-HCl increased continuously with respect to specific charges for the entire duration of electrolysis treatment. The decay of MET-HCl depended on the current density, and the degradation was observed increasing from 87.24 to 95.06% as current density increased from 0.67 to 0.93 mA/cm^2; corresponding specific charge being 1.5 and 2.1 Ah/L, respectively. The degradation increased only marginally from 95.06 to 95.20% as current density increased from 0.93 to 1.16 mA/cm^2 at a corresponding specific charge of 2.6 Ah/L. The pseudo-first-order rate constant was found to increase when current density increased from 0.67 to 0.93 mA/cm^2, but it decreased with a further increase in current density from 0.93 to 1.16 mA/cm^2. These are shown in Table 2. This highlights the significance of parasitic reactions, notably oxygen evolution, and loss of persulfate ions if the current density exceeds a threshold.

To quantify MET-HCl mineralization on SS anode, relative TOC concentration was plotted against Specific charges at different current densities and shown in Fig. 5c. Fig. 5d shows linear regression of ln (TOC_t/TOC_0) to Specific charge with varying current density and the correlation coefficients in each case. This confirms adherence to pseudo- first order kinetics for mineralization on SS anode as well. Mineralization of MET-HCl depended on

Table 2: First order rate kinetics of combined electro-oxidation & electro-coagulation of MET-HCl at SS anode.

Current density (mA/cm^2)	Na_2SO_4 concentration (ppm)	value of rate constant k (L/Ah)
Mineralization		
0.67	50	1.1729
0.93	50	1.4192
1.16	50	0.8272
0.93	75	2.3818
0.93	100	1.7833
Degradation		
0.67	50	1.4158
0.93	50	1.4834
1.16	50	1.2080
0.93	75	2.4331
0.93	100	2.5351

the current density. It increased from 80.84 to 93.80% with current density increasing from 0.67 to 0.93 mA/cm^2. A commensurate increase in the pseudo-first-order rate constant was observed, as shown in Table 2. The increase in current density could enhance the formation of ·OH by eq^n (1) and thus increase the mineralization of MET-HCl. Beyond this, current density had a negative influence on the mineralization of MET-HCl. We observed a decrease in mineralization from 93.80 to 86.63% when current density increased from 0.93 to 1.16 mA/cm^2. This is also reflected in the corresponding drop in the pseudo-first-order rate constant. These are shown in Table 2. Here it is important to note that when the current density exceeds a certain value, in this case from 0.93 to 1.16 mA/cm^2, the TOC removal did not enhance. It is because of the oxygen evolution reaction, which on one hand wasted the hydroxyl radicals and on the other masked the active sites on the anode surface [43]. Also, a part of the specific charge is used in the oxidation of Fe to Fe^{2+} according to eq^n (12). Consequently the mediated oxidation by electro-generated HO· from the decomposition of the water is less favored as compared to the mediated oxidation by electro-generated $S_2O_8^{2-}$ and $SO_4^{\cdot-}$, from Na_2SO_4. Due to this complete oxidation of the organic matter into CO_2 does not occur.

Fig. 5e shows the effect of the current density on the EC as a function of Specific charge (Ah/L) for the SS anode. At each current density, EC increased continuously with respect to specific charges for the entire duration of electrochemical treatment. As current density increased from 0.67 to 0.93 and then to 1.16 mA/cm^2 the EC also increased from 711 to 944.31 and further to 1480.99 kWh/kg TOC. Higher current density also accelerated the side reactions such as the formation of O_2, leading to a larger proportion of specific charge being consumed on these side reactions. This is reflected in the form of increased EC [45-46].

Fig. 5f shows the effect of the current density on the MCE as a function of Specific charge (Ah/L) for the SS anode. MCE decreased with the specific charge at each current density and at a comparable specific charge the MCE decreased with increasing current density. The reduction of MCE with specific charge could be related to the production of recalcitrant intermediate products [47-48]. As current density increased from 0.67 to 0.93 mA/cm^2 the final MCE decreased from 22.71 to 18.82% after corresponding specific charge values of 1.5 and 2.1 Ah/L, respectively. MCE further dropped to 14.04% as current density increased to 1.16 mA/cm^2 at a corresponding specific charge of 2.6 Ah/L. At higher potentials associated with higher current densities, a larger proportion of specific charge is consumed in oxygen evolution compared to the generation of hydroxyl radicals [47] and consequently MCE is also decreased.

Influence of supporting electrolyte concentration

The effect of Na_2SO_4 concentration on the MET-HCl decay is presented in Fig. 6a as relative concentration plotted against the Specific charge for the SS anode. Fig. 6b presents the linear regression plots between ln (C_t/C_o) and Specific charge as a means to validate pseudo-first-order kinetics at different Na_2SO_4 concentrations. R^2 values are sufficiently high for all regressions. At each Na_2SO_4 concentration, degradation of MET-HCl increased continuously with a specific charge. The decay of the MET-HCl depended on the Na_2SO_4 concentration, and the degradation increased from 95.06 to 99.20% with an increase in Na_2SO_4 concentration from 50 to 75 ppm. A marginal increase in degradation was further observed, from 99.20 to 99.48% - almost complete degradation – as Na_2SO_4 concentration increased from 75 to 100 ppm. Improvement in solution conductivity and the resulting ease of movement of ions is primarily responsible for this increase. In addition, higher concentrations of Na_2SO_4 also generate additional amounts of the oxidants $S_2O_8^{2-}$, and $SO_4^{\bullet-}$. The pseudo first order rate constant was found increasing with Na_2SO_4 concentration. These rate constants are shown in Table 2.

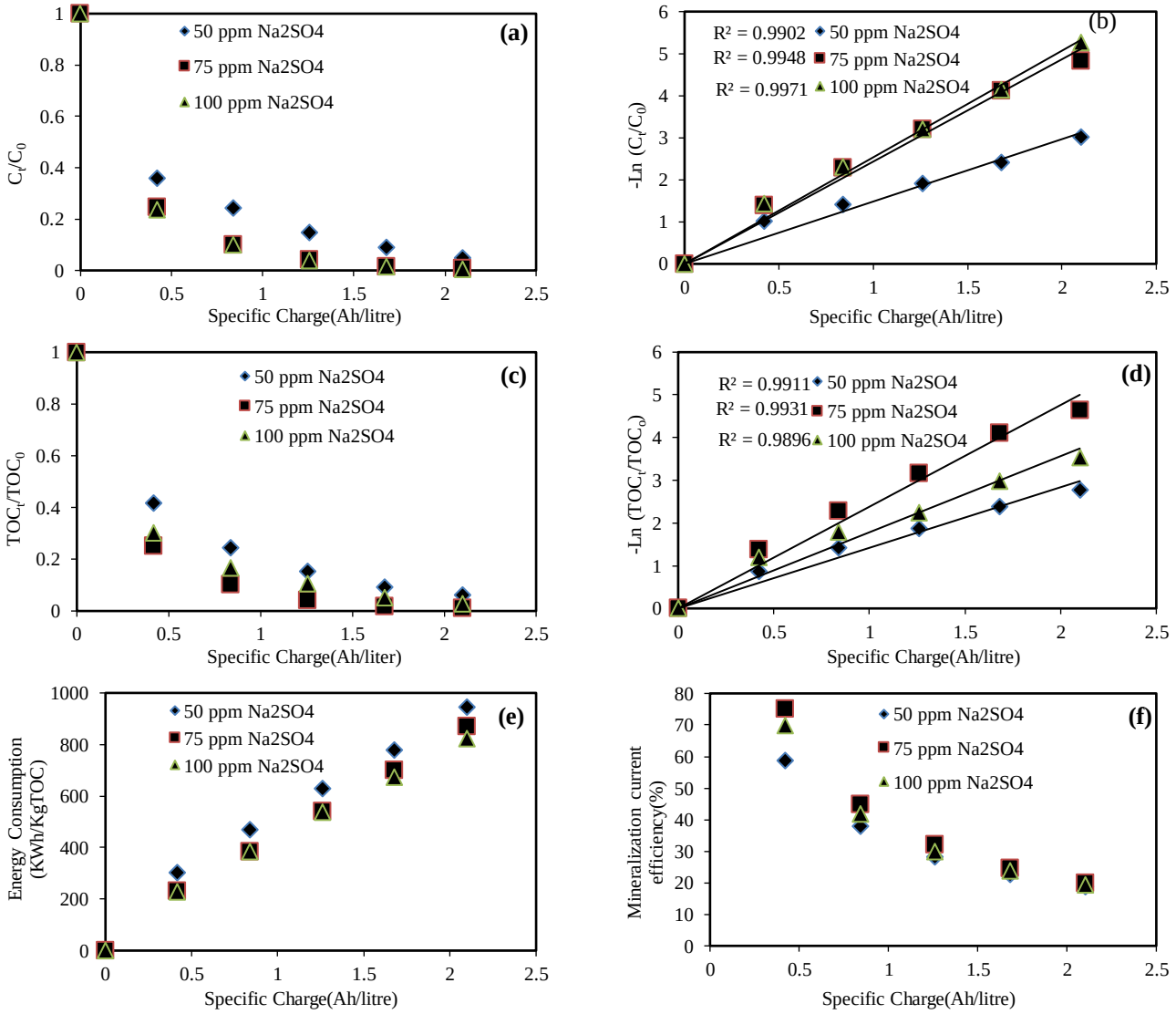

Fig. 6: Effect of Na_2SO_4 concentration and specific charge (Ah/L) on the combined electro-oxidation and electro-coagulation of MET-HCl on SS anode (a) relative MET-HCl concentration (b) ln (C_t/C_0) (c) relative TOC concentration (d) ln(TOC_t/TOC_0) (e) EC (f) MCE. Conditions: 50 ppm MET-HCl, Current density 0.93 mA/cm^2

Mineralization, as measured by relative TOC concentration, is shown as a function of Specific charge for different Na_2SO_4 concentrations in Fig. 6c. Plots of pseudo-first-order integral rate equations are shown in Fig. 6d. Mineralization was found to increase from 93.80 to 99.04% – almost complete mineralization – as Na_2SO_4 concentration was increased from 50 to 75 ppm. The corresponding increase in the pseudo-first-order mineralization rate constant is reported in Table 2. But mineralization decreased from 99.04 to 97.11% with Na_2SO_4 concentration increasing further to 100 ppm with a corresponding drop in pseudo-first-order rate constant. This trend of first increase and then decrease in TOC abatement is linked to competitive electro-oxidation of SO_4^{2-} and water at the anode. Increased concentration of SO_4^{2-} in the system is a trade-off between higher solution conductivity and lower water splitting. The first facilitates the movement of ions while the second reduces the hydroxyl ion concentration.

Fig. 6e shows the effect of the Na_2SO_4 concentration on the EC as a function of the specific charge for the SS anode. Irrespective of Na_2SO_4 concentration, EC increased continuously with respect to specific charge. As Na_2SO_4 concentration increased from 50 to 75 ppm, the EC decreased from 944.31 to 870.98 kWh/ kg TOC. Similarly

when Na_2SO_4 concentration was increased from 75 to 100 ppm, the EC further decreased from 870.98 to 822.71 kWh/kgTOC. Higher the Na_2SO_4 concentration, lower the cell voltage required to maintain a given current density. This translates into reduced EC.

Fig. 6f shows the effect of the Na_2SO_4 concentration on the MCE as a function of Specific charge (Ah/L) for the SS anode. Initially, there was an increase in MCE from 18.82 to 19.87% as Na_2SO_4 concentration increased from 50 to 75 ppm. Thereafter, a small decrease in MCE to 19.48% happened at higher Na_2SO_4 concentration of 100 ppm. On one hand, higher Na_2SO_4 concentration supressed the generation of hydroxyl radicals as SO_4^{2-} would compete for the transferred charge with the water splitting reaction. On the other hand, more and more hydroxyl radicals were formed and destroyed through eq^n (9), (10) and (11) when the Na_2SO_4 concentration increased. That is why this radical's lesser proportion was available for the reaction with organics [47] and consequently MCE was also decreased.

Comparison of electro-oxidation on Ti/DSA anode with combined electro-oxidation and electro-coagulation on SS anode

In case of electro-oxidation at Ti/DSA anode, MET-HCl is oxidized by hydroxyl radicals, persulfate ions and sulfate radicals whereas in combined electro-oxidation and electro-coagulation on SS anode, oxidation of MET-HCl is complemented by its removal by ferrous and ferric ions.

In the case of electro-oxidation at Ti/DSA anode the degradation of 50 ppm MET-HCl in 50 ppm of Na_2SO_4 background solution increased from 85.56 to 90.46% as current density increased from 0.67 to 1.16 mA/cm^2 after 2.6 Ah/L of Specific charge. In comparison, in combined electro-oxidation and electro-coagulation on SS anode, the degradation was observed to increase from 87.24 to 95.20% as current density increased from 0.67 to 1.16 mA/cm^2 after 2.6 Ah/L of Specific charge. The higher degradation can be attributed to the release of Fe^{2+} and Fe^{3+} from SS anode which acted as a coagulant agent in the electro-coagulation. A similar trend was noticed for mineralization as well. For the electro-oxidation at Ti/DSA anode, an increase in mineralization from 55.27 to 70.64% was noticed when the current density increased from 0.67 to 0.93 mA/cm^2. However mineralization of MET-HCl was observed to decrease from 70.64 to 68.16% when current density increased from 0.93 mA/cm^2 to 1.16 mA/cm^2. Similarly, for combined electro-oxidation and electro-coagulation on SS anode, mineralization was observed increasing from 80.84 to 93.80% when current density increased from 0.67 to 0.93 mA/cm^2 but mineralization of MET-HCl was observed decreasing from 93.80 to 86.63% when current density increased from 0.93 to 1.16 mA/cm^2. For all current densities, the mineralization is more in the case of the combined process due to the electro-generation of Fe^{2+} which leads to coagulation of the pollutants. This combined with the electro-oxidation, facilitated by hydroxyl radicals and other oxidants like per sulfate ion and sulfate radicals, results in higher mineralization. Under comparable conditions, EC for electro-oxidation at Ti/DSA anode increased from 1017.46 to 2281.90 kWh/kg TOC whereas for combined electro-oxidation and electro-coagulation on SS anode, it increased from 711 to 1480.99 kWh/kg TOC. Thus, EC is lower for combined electro-oxidation and electro-coagulation compared to electro-oxidation alone. The same is true for MCE and for similar reasons. Under similar conditions, MCE for electro-oxidation at Ti/DSA anode decreased from 15.52 to 11.04%, whereas for combined electro-oxidation and electro-coagulation on SS anode, it decreased from 22.71 to 14.04%.

Electrochemical remediation of metformin is not reported in technical literature. Therefore the results obtained in this study cannot be directly compared with the previous work of other researchers. For the closest comparison, metformin was degraded and mineralized by the electro-Fenton process and degradation and mineralization of 89.25 and 68.42% respectively, are reported with energy consumption of 1.43 Wh/L [12].

CONCLUSIONS

In the present experimental investigation, the degradation and mineralization of the antidiabetic drug MET-HCl in synthetic wastewater was studied by electro-oxidation and combined electro-oxidation and electro-coagulation on Ti/DSA and SS anode respectively, in a batch operation. The electrochemical degradation and mineralization of MET-HCl depended on the anode type. Both Ti/DSA and SS are capable of degrading and mineralizing MET-HCl. However, MET-HCl degradation was 94.88% on Ti/DSA, which was lower than the 99.48% degradation achieved with SS anode. Mineralization (70.64%) was also lower with Ti/DSA compared to

mineralization with SS (99.04%). Combined electro-oxidation and electro-coagulation on SS anode were energetically more favored than electro-oxidation on Ti/DSA reflected in the EC of 870.98 and 2081.56 kWh/kgTOC, respectively, in the two processes. SS anode was more efficient than Ti/DSA in utilizing the transferred electrolytic charge towards pollutant mineralization in aqueous matrix as illustrated by the corresponding MCE of 18.82 and 14.17%. Degradation and mineralization processes followed pseudo-first-order kinetics on both the anodes. The addition of Na_2SO_4 as a supporting electrolyte in moderate amounts could facilitate degradation and mineralization while lowering EC as well.

Acknowledgments: All assistance obtained is acknowledged.

Received: Oct. 17, 2021 ; Accepted: Jan. 10, 2022

References

[1] Viollet B., Guigas B., Garcia N.S., Leclerc J., Foretz M., Andreelli F., Cellular and Molecular Mechanisms of Metformin: An Overview, *Clin. Sci.*, **122:** 253 (2012).

[2] Zhu S., Liu Y.G., Liu S.B., Zeng G.M., Jiang .LH., Tan X.F., Zhou L., Zeng W., Li T.T., Yang C.P., Adsorption of Emerging Contaminant Metformin using Graphene Oxide, *Chemosphere*, **179:** 20 (2017).

[3] Orona-Navar C., Garcia-Morales R., Rubio-Govea R., Mahlknecht J., Hernandez-Aranda R.I., Ramirez J.G., Nigam K.D.P., Ornelas-Soto N., Adsorptive Removal of Emerging Pollutants from Groundwater by Using Modified Titanate Nanotubes, *Journal of Environmental Chemical Engineering*, **6:** 5332 (2018).

[4] Lesser L.E., Mora A., Moreau C., Mahlknecht J., Hernández-Antonio A., Ramírez A.I., Barrios-Piña H., Survey of 218 Organic Contaminants in Groundwater Derived from the world's Largest Untreated Wastewater Irrigation System: Mezquital Valley, Mexico, *Chemosphere*, **198:** 510 (2018).

[5] Oliveira T.S., Murphy M., Mendola N., Wong V., Carlson D., Waring L., Characterization of Pharmaceuticals and Personal Care Products in Hospital Effluent and Waste Water Influent/Effluent by Direct-Injection LC-MS-MS, *Sci. Total Environ*, **518–519:** 459 (2015).

[6] Scheurer M., Michel A., Brauch H.J., Ruck W., Sacher F., Occurrence and Fate of the Antidiabetic Drug Metformin and its Metabolite Guanylurea in the Environment and During Drinking Water Treatment, *Water Res.*, **46:** 4790 (2012).

[7] Kim M., Guerra P., Shah A., Parsa M., Alaee M., Smyth S.A., Removal of Pharmaceuticals and Personal Care Products in a Membrane Bioreactor Wastewater Treatment Plant, *Water Sci. Technol*, **69(11):** 2221 (2014).

[8] USEPA, Targeted National Sewage Sludge Survey Sampling and Analysis Technical Report (Vol. EPA-822-R-), *USEPA*, Washington, DC, (2009).

[9] Oosterhuis M., Sacher F., Laak T.L.T., Prediction of Concentration Levels of Metformin and other High Consumption Pharmaceuticals in Wastewater and Regional Surface Water Based on Sales Data, *Sci. Total. Environ.*, **442:** 380 (2013).

[10] Trautwein C., Berset J.D., Wolschke H., Kümmerer K., Occurrence of the Antidiabetic Drug Metformin and its Ultimate Transformation Product Guanylurea in Several Compartments of the Aquatic Cycle, *Environ. Int.* ,**70:** 203 (2014).

[11] Ghoshdastidar A.J., Fox S., Tong A.Z., The Presence of the Top Prescribed Pharmaceuticals in Treated Sewage Effluents and Receiving Waters in Southwest Nova Scotia, Canada, *Environ. Sci. Pollut. Res.*, **22:** 689 (2015).

[12] Aseman-Bashiz E., Sayyaf H., Metformin Degradation in Aqueous Solutions by Electro-Activation of Persulfate and Hydrogen using Natural and Synthetic Ferrous Ion Sources, *Journal of Molecular liquids*, **300:** 112285 (2020).

[13] Cunningham V.L., "Pharmaceuticals in the Environment: Sources, Fate, Effects and Risks", Springer Berlin, (2008).

[14] Nikolaou A., Meric S., Fatta D., Occurrence Patterns of Pharmaceuticals in Water and Wastewater Environments, *Anal. Bioanal. Chem.*, **387(4):** 1225 (2007).

[15] Benotti M.J., Brownawell B.J., Distributions of Pharmaceuticals in An Urban Estuary During both Dry- and Wet-Weather Conditions, *Environ. Sci. Technol.*, **41:** 5795 (2007).

[16] Debska J., Kot-Wasik A., Namiesnik J., Fate and Analysis of Pharmaceutical Residues in the Aquatic Environment, *Crit. Rev. Anal. Chem*, **34(1):** 51 (2004).

[17] Joss A., Siegrist H., Ternes T.A., Are We About to Upgrade Wastewater Treatment for Removing Organic Micropollutants? *Water Sci. Technol*, **57(2):** 251 (2008).

[18] Eggen T., Asp T.N., Grave K., Hormazabal V., Uptake and Translocation of Metformin: Ciprofloxacin and Narasin in Forage- and Crop Plants, *Chemosphere*, **85:** 26 (2011).

[19] Eggen T., Lillo C., Antidiabetic II drug Metformin in Plants: Uptake and Translocation to Edible Parts of Cereals Oily Seeds, Beans, Tomato, Squash, Carrots, and Potatoes, *J. Agric. Food. Chem*, **60**: 6929 (2012).

[20] Hai F.I., Yang S., Asif M.B., Sencadas V., Shawkat S., Sanderson-Smith M., Gorman J., Xu Z.Q., Yamamoto K., Carbamazepine as a Possible Anthropogenic Marker in Water: Occurrences, Toxicological Effects, Regulations and Removal by Wastewater Treatment Technologies, *Water*, **10(2):** 107 (2018).

[21] Zainab A., Zainab pP., Electrochemical Sensor Based on Nanocomposite of Multi-Walled Carbon Nano-Tubes (MWCNTs)/TiO_2/Carbon Ionic Liquid Electrode Analysis of Acetaminophen in Pharmaceutical Formulations, *Iran. J. Chem. Chem. Eng. (IJCCE)*, **40**: 1030-1041 (2021).

[22] Zehra A.B., Aghbalaghi Z.A., Electrochemical Determination Venlafaxine at NiO/GR Nanocomposite Modified Carbon Paste Electrode, *Iran. J. Chem. Chem. Eng. (IJCCE)*, **40:** 1030-1041 (2021).

[23] Niemuth N.J., Klaper R.D., Emerging Wastewater Contaminant Metformin Causes Intersex and Reduced Fecundity in Fish, *Chemosphere*, **135:** 38 (2015).

[24] Poursat B.A.J., spanning R.J.M.V., Braster M., Helmus R., Biodegradation of Metformin and its Transformation Product, Guanylurea, by Natural and Exposed Microbial Communities, *Ecotoxicol. Environ. Saf.*, **182:** 109414 (2019).

[25] Trautwein C., Kümmerer K., Incomplete Aerobic Degradation of the Antidiabetic Drug Metformin and Identification of the Bacterial Dead-End Transformation Product Guanylurea, *Chemosphere*, **85**:765 (2011).

[26] Cahill J.D., Furlong E.T., Burkhardt M.R., Kolpin D., Anderson L.G., Determination of Pharmaceutical Compounds in Surface- and Ground-Water Samples by Solid-Phase Extraction and High-Performance Liquid Chromatography-Electrospray Ionization Mass Spectrometry, *J. Chromatogr. A*, **1041:** 171 (2004).

[27] Bones J., Thomas K., Nesterenko P.N., Paull B., On-Line Preconcentration of Pharmaceutical Residues from Large Volume Water Samples using Short Reversed-Phase Monolithic Cartridges Coupled to LC-UV-ESI-MS, Talanta, **70:** 1117 (2006).

[28] Chelliapan S., Wilby T., Sallis P.J., Performance of an Up-Flow Anaerobic Stage Reactor (UASR) in the Treatment of Pharmaceutical Wastewater Containing Macrolide Antibiotics, *Water Res.*, **40:** 507(2006).

[29] Writer J.H., Ferrer I., Barber L.B., Thurman E.M., Widespread Occurrence of Neuroactive Pharmaceuticals and Metabolites in 24 Minnesota Rivers and Wastewaters, *Sci. Total Environ.*, **461–462:** 519 (2013).

[30] Castiglioni S., Bagnati R., Fanelli R., Pomati F., Calamari D., Zuccato E., Removal of Pharmaceuticals in Sewage Treatment Plants in Italy, *Environ. Sci. Technol.*, **40:** 357 (2006).

[31] Dodd M.C., Kohler H.E., Gunten U.V., Oxidation of Antibacterial Compounds by Ozone and Hydroxyl Radical: Elimination of Biological Activity During Aqueous Ozonation Processes Oxidation of Antibacterial Compounds by Ozone and Hydroxyl Radical: Elimination of Biological Activity during Aqueo, *Environ. Sci. Technol.*, **43:** 2498 (2009).

[32] Pelaez M., Nolan N.T., Pillai S.C., Seery M.K., Falaras P., Kontos A.G., Dunlop P.S.M., Hamilton J.W.J., Byrne J.A., O'Shea K., Entezari M.H., Dionysiou D.D., A Review on the Visible Light Active Titanium Dioxide Photocatalysts for Environmental Applications, *Appl. Catal. B Environ.*, **125:** 331 (2012).

[33] Tabish T.A., Pranjol M.Z.I., Jabeen F., Abdullah T., Latif A., Khalid A., Ali M., Hayat H., Winyard P.G., Whatmore J.L., Zhang S., Investigation into the Toxic Effects of Graphene Nanopores on Lung Cancer Cells and Biological Tissues, *Appl. Mater. Today*, **12:** 389 (2018).

[34] Sattarahmady N.,Heli H., Faramarza F., Nickel Oxide Nanotubes-Carbon Microparticles/Nafion Nanocomposite for the Electrooxidation and Sensitive Detection of Metfomin, *Talanta*, **82:** 1126 (2010).

[35] Jeong J., Lee J., Electrochemical Oxidation of Industrial Wastewater with the Tube Type Electrolysis Module System, *Sep. Purif. Technol*, **84:** 35 (2012).

[36] Keshipour S., Faraji M., Aboozari Asl P, Sonochemical Fabrication of Pd/TiO_2-Nanotubes/Ti Plate as a Green Catalyst for Oxidation of Alkylarenes and Benzyl Alcohols, *J. Iran. Chem. Soc.*, **16:** 1423-1429 (2019).

[37] Keshipour S., Alizadeh S.M., Nickel Phthalocyanine@ Grapheme Oxide/TiO_2 as an Efficient Degradation Catalyst of Formic Acid Toward Hydrogen Production, *Sci. rep.*, **11:** 16148 (2021).

[38] Keshipour S., Alizadeh S.M., Razeghi M.H., Copper Phthalocyanine@Graphene Oxide as a Cocatalyst of TiO_2 in Hydrogen Generation, *J. Phys. Chem. Solids*., **161:** 110434 (2022).

[39] Ghatak H. R., Comparative Removal of Commercial Diclofenac Sodium by Electro-Oxidation on Platinum Anode and Combined Electro Oxidation and Electro-Coagulation on Stainless Steel Anode, *Environ. Technol.*, **35(19):** 2483 (2014).

[40] Ghatak H.R., Simulated Process Integration of Wastewater Electrooxidation with Recuperated Micro Gas Turbine for Energy Recovery, *Int. J. Hydrog. Energy*, **45(56):** 31466 (2020).

[41] Silva S.W.D., Navarro E.M.O., Rodrigues M.A.S., Bernardes M.A., Herranz V.P., Using p-Si/BDD Anode for the Electrochemical Oxidation of Norfloxacin, *J. Electroanal. Chem.*, **832:** 112 (2019).

[42] Davis J., Baygents J.C., Farrell J., Understanding Persulfate Production at Boron Doped Diamond Film Anodes, *Electrochimica Acta*, **150:** 68 (2014)

[43] Samet Y., Agengui L., Abdelhédi R., Electrochemical Degradation of Chlorpyrifos Pesticide in Aqueous Solutions by Anodic Oxidation at Boron-Doped Diamond Electrodes, *Chem. Eng. J.*, **161:** 167 (2010).

[44] Cai J., Zhou M., Pan Y., Lu X., Degradation of 2,4-Dichlorophenoxyacetic Acid by Anodic Oxidation and Electro-Fenton using BDD Anode:Influencing Factors and Mechanism, *Sep. Purif. Technol.*, **230:** 115867 (2020).

[45] You S., Liu B., Gao L., Wang Y., Tang C.Y., Huang Y., Ren N., Monolithic Porous Magnéli-Phase Ti_4O_7 for Electro-Oxidation Treatment of Industrial Wastewater, *Electrochim. Acta*, **214:** 326 (2016).

[46] Martinez-Huitle C.A., Rodrigo M.A., Sires I., Scialdone I., Single and Coupled Electrochemical Processes and Reactors for the Abatement of Organic Water Pollutants: A Critical Review, *Chem. Rev.*, **115:** 13362 (2015).

[47] Hamza M., Abdelhedi R., Brillas E,, Sirés I., Comparative Electrochemical Degradation of the Triphenylmethane Dye Methyl Violet with Boron-Doped Diamond and Pt Anodes, *J. Electroanal. Chem*, **627:** 41 (2009).

[48] Guinea E., Garrido J.A., Rodríguez R.M., Cabot P.L., Arias C., Centellas F., Brillas E., Degradation of the Fluoroquinolone Enrofloxacin by Electrochemical Advanced Oxidation Processes based on Hydrogen Peroxide Electrogeneration, *Electrochim.Acta*, ***55*:** 2101 (2010).